PROTEIN STRUCTURE REPORT

The zinc finger domain of RING finger protein 141 reveals a unique RING fold

Kazuhide Miyamoto,* Airi Uechi, and Kazuki Saito

Department of Pharmaceutical Health Care, Faculty of Pharmaceutical Sciences, Himeji Dokkyo University, Hyogo, Japan

Received 7 April 2017; Accepted 15 May 2017
DOI: 10.1002/pro.3201
Published online 25 May 2017 proteinscience.org

Abstract: Human RING finger protein 141 (RFP141) is a germ cell-specific transcription factor during spermatogenesis. We synthesized a compact construct encoding the C-terminal zinc finger of RFP141 (RFP141C peptide). Herein we determined the solution structure of the RFP141C peptide by nuclear magnetic resonance (NMR). Moreover, NMR data and the chemical modification of cysteine residues demonstrated that the RFP141C peptide binds to two zinc atoms in a cross-brace arrangement. The Simple Modular Architecture Research Tool database predicted the structure of RFP141C as a RING finger. However, the actual structure of the RFP141C peptide adopts an atypical compact C_3HC_4-type RING fold. The position and range of the helical active site of the RFP141C structure were elucidated at the atomic level. Therefore, structural analysis may allow RFP141C to be used for designing an artificial RING finger possessing specific ubiquitin-conjugating enzyme (E2)-binding capabilities.

Keywords: RING finger protein 141; NMR structure; zinc finger; peptide; artificial RING finger

Introduction

Cross-brace zinc finger motifs, such as RING,[1] PHD,[2] FYVE,[3] and ZZ[4] fingers, have a common zinc-binding structural feature. Apart from this shared structure, each finger is unique and has a specific biological function.[4] For example, RING fingers function as ubiquitin (Ub)-ligating (E3) enzymes in protein ubiquitination,[5] transferring activated Ub to the lysine residues of substrates.[6,7] Most E3 RING fingers possess a helical region (active site), an essential key for their specific Ub-conjugating enzyme (E2)-binding capabilities for ubiquitination.[1,8,9] On the other hand, PHD, FYVE, and ZZ fingers cannot promote protein ubiquitination because they lack functional helical structures.[2,3,10] Recently, we reported the "α-helical region substitution" method for creating an artificial RING finger (ARF) that has E3 activity and ubiquitinates itself without a substrate. The use of an ARF allows the simplified detection of E2 activities in ubiquitination reactions.[11] Because E2 activities are associated with various diseases, such as leukemia,[12] lung cancer,[13] and breast cancer,[14] the use of ARFs may lead to novel cancer diagnostic techniques. ARFs are engineered by grafting the active site of the RING finger onto other cross-brace zinc motifs.[15] When a PHD finger is utilized as a scaffold, grafting confers the E3 activity of a RING finger to the PHD finger.[16,17] There is growing interest to extend this method to various RING fingers; therefore, we felt the need to elucidate their atomic structures to identify appropriate positions for the grafting of active sites. Human RING

Disclosure: The authors declare no competing financial interests.

Grant sponsor: Grant-in-Aid for Scientific Research and the Nakatani Foundation; Grant number: KAKENHI 17K05942.

*Correspondence to: K. Miyamoto; Department of Pharmaceutical Health Care, Faculty of Pharmaceutical Sciences, Himeji Dokkyo University, Hyogo 670-8524, Japan. E-mail: miyamoto@himeji-du.ac.jp

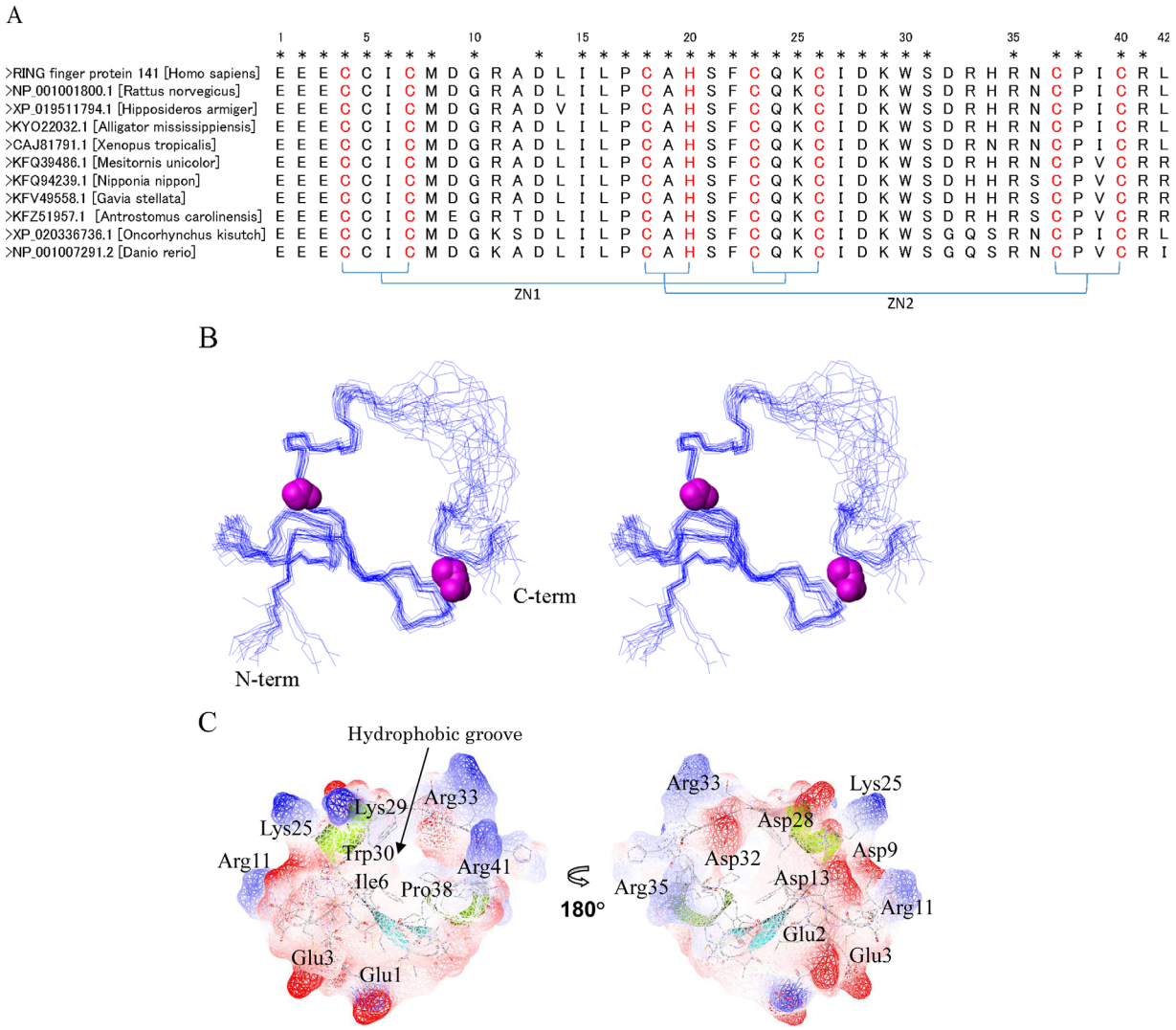

Figure 1. A: Sequence alignment of the amino acid sequence of the C-terminal zinc finger of human RING finger protein 141 (RFP141C). ZN1 and ZN2 depict the two zinc-binding sites in a cross-brace arrangement. Zinc ligands are shown in red. Stars indicate the well-conserved residues among homologs. B: Stereoview illustrating the trace of the backbone atoms for the ensemble of the 20 lowest energy structures (residues Glu1–Leu42). Zinc atoms are shown in magenta. C: Surface representation and ribbon diagram of the RFP141C peptide illustrating the side chains. Surface representation was calculated using Discovery Studio 2.1. The α-helical and β-sheet regions are shown in green and blue, respectively.

finger protein 141 (RFP141) consists of 230 amino acids and is considered to serve as a germ cell-specific transcription factor during spermatogenesis.[18] The Simple Modular Architecture Research Tool (SMART) database predicted the C-terminal zinc finger of RFP141 (RFP141C) as a RING finger. In the present study, to augment the RING finger protein list applicable to design an ARF, we investigated the solution structure of RFP141C via nuclear magnetic resonance (NMR). However, structural analysis revealed that RFP141C adopts an atypical RING fold in a cross-brace arrangement.

Results and Discussion

The RFP141C peptide binds to two zinc atoms

The RFP141C peptide was prepared by peptide synthesis (Fig. 1). The zinc-binding capabilities of the RFP141C peptide were assayed using the cysteine modification of *p*-hydroxymercuribenzoic acid (PHMB) and 4-(2-pyridylazo) resorcinol (PAR).[19–21] The concentration of the RFP141C peptide was 2.0 μ*M*, and the absorbance (A) of the zinc–PAR complex was 0.30 at 500 nm. The estimated concentration of the zinc ions was 4.5 μ*M*. Therefore, the zinc:protein ratio was 2.25 at 20°C, indicating that the RFP141C peptide binds to two zinc atoms.

Resonance assignments and overall structure

NMR assignments for the $^{13}C/^{15}N$-labeled RFP141C peptide were performed using conventional heteronuclear methods.[22] Backbone resonance assignments were complete, except for the amide protons of Glu1 and Leu42. The residues Cys4, Cys7, Cys18, Cys23, Cys26, Cys37, and Cys40 have been identified as

Table I. Summary of Structure Statistics of the RFP141C Peptide[a]

NOE upper distance restraints	
Total	511
Short-range ($\|i-j\| = 1$)	308
Medium range ($1 < \|i-j\| < 5$)	66
Long rage ($\|i-j\| \geq 5$)	137
CYANA target function value	0.01 Å^2
Distance constraints violations	
Number > 0.1 Å	0
Maximum	0.02 Å
PROCHECK Ramachandran plot analysis[b]	
Residues in most favored regions	59.8%
Residues in additionally allowed regions	34.7%
Residues in generously allowed regions	4.3%
Residues in disallowed regions	1.2%
RMS deviation to the average coordinates[b]	
Backbone atoms	0.55 Å
Heavy atoms	1.14 Å

[a] Except for the number of constraints, average values given for the set of 20 conformers with the lowest energy value.
[b] The values were calculated for residues 3–30 and 37–41.

zinc-binding ligands because the spectra of their C_β atoms are between 27.0 and 30.0 ppm.[23] The spectrum of the $C_{\delta 2}$ atom of the His20 residue is less than 122 ppm, which indicated its $N_{\epsilon 2}$–H tautomer as a possible zinc-binding ligand.[24] NOE connectivities between the H_β protons of Cys4, Cys7, Cys23, and Cys26 showed that these residues gather to form one of the two zinc-binding sites. All zinc-binding ligands were completely conserved among various species of RFP141 (Fig. 1). Our finding indicated that the RFP141C peptide adopts C_3HC_4-type zinc coordination in a cross-brace arrangement. Therefore, the constraints for the tetrahedral zinc coordination were added as distance constraints for structure calculations. The solution structure of the RFP141C peptide was calculated using CYANA[25] and Discovery Studio 2.1 (Accelrys Software).[15] Fitting of the 20 lowest energy structures of the RFP141C peptide is shown in Figure 1(B). The statistics of the ensemble structure and distance constraints for the RFP141C peptide are summarized in Table I. The well-ordered region (Glu3–Trp30 and Cys37–Arg41) are superimposed over the backbone (N, C^α, and C′) and nonhydrogen atoms, with root mean square (RMS) deviations of 0.55 and 1.14 Å, respectively. The loop region of residues Ser31–Asn36 was not well ordered. A Ramachandran plot checked by PROCHECK-NMR[26] showed the quality of the structures, that is, 94.5% of the well-ordered region was within the most favored regions and additionally allowed regions. The Connolly surface of the RFP141C peptide was calculated by Discovery Studio 2.1 [Fig. 1(C)]. Residues Ile6, Trp30, and Pro38 contributed to the formation of a hydrophobic shallow groove surrounded by the positively charged residues Lys29, Arg33, and Arg41. On the opposite side, the negatively charged residues Glu2, Glu3, Asp9, Asp13, Asp28, and Asp32 formed the highly acidic surface of the RFP141C peptide. NMR results showed that the RFP141C peptide possesses two α-helices and one antiparallel β-sheet (α1: Gln24–Lys29, α2: Pro38–Arg41, β1: Ile15-Leu16, β2: His20-Ser21) [Fig. 2(A)]. The residues Leu16, Phe22, and Ile27 formed the hydrophobic core for proper folding. Taken together, our data indicated that the RFP141C peptide is a compact zinc-binding structure in a cross-brace arrangement.

Comparison with other RING structures

The structure of RFP141C was predicted to be a RING fold through the SMART database query. RING structures are classified into the four categories: I-a, I-b, II-a, and II-b. It was found that the RING structure of RFP141C belongs to category I-b, but not category I-a.[9] The typical RING structure of

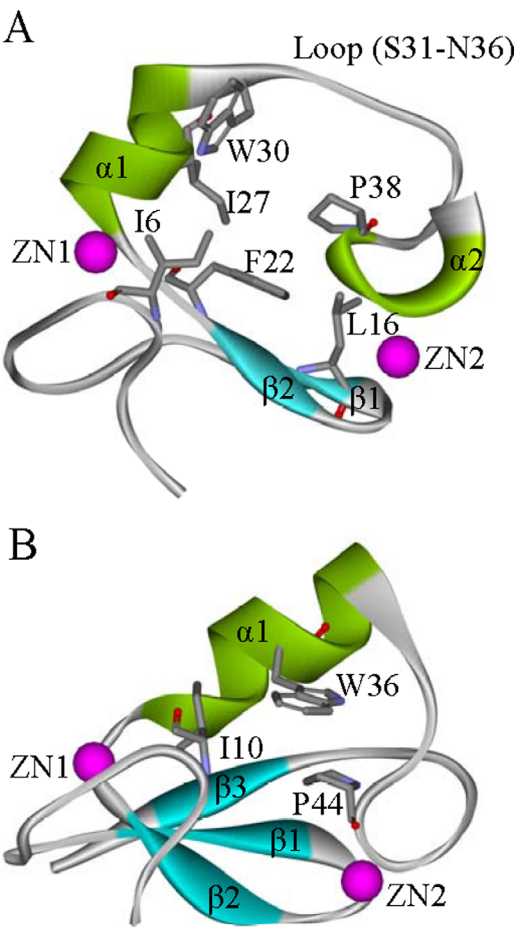

Figure 2. Structural comparisons between other RING structures and the RFP141C peptide. Ribbon diagrams of (A) the lowest energy structure of the RFP141C peptide showing the heavy atoms of the side chains of the hydrophobic core and hydrophobic groove-forming residues. (B) The RING structure of the equine herpes virus protein showing the hydrophobic groove-forming residues. Zinc atoms, β-strands, and α-helices are shown in magenta, blue, and green, respectively.

category I-b from the equine herpes virus protein (EHVP)[27] is shown in Figure 2(B). The data indicated that the structure adopts a cross-braced zinc-binding motif and possesses antiparallel β-sheet and α-helical structures. The structure of RFP141C lacks a β3-strand, corresponding to that of EHVP; therefore, RFP141C adopts a compact RING fold. It seems that the β3-strand of RING structures is a dispensable part for proper folding. The flexible loop (Ser31–Asn36) of RFP141C is a unique feature that does not exist in the RING structure of EHVP. The residues Ile10, Trp36, and Pro44 of EHVP form a similar hydrophobic shallow groove to those of RFP141C. Most RING structures have a hydrophobic shallow groove for E2-binding during ubiquitination.[1,8,9] For specific E2-binding capabilities, the residue Trp is a crucial determination factor.[9] Category I-b RING fingers possessing the residue Trp promote ubiquitination with E2 (UbcH4 or UbcH7).[28,29] Therefore, it is tempting to speculate that RFP141C possesses specific E3 activities and transfer activated Ub from E2 to substrate molecules in the ubiquitination pathway.

Cross-brace structure for creating ARFs

The use of ARFs enables the monitoring of E2 activities in ubiquitination and also allows for the assessment of the pathological conditions of acute promyelocytic leukemia-derived NB4 cells.[11,12] When designing ARFs, the helical region (active site) of the RING finger is grafted onto other cross-brace zinc motifs as mentioned previously. In this work, the position and range of the α1-helix as the active site of RFP141C were elucidated at the atomic level. Grafting of the α1-helix may lead to the creation of a novel ARF that functions as an E3 ligase during ubiquitination. Thus, the present structural study provides an important insight into the creation of ARFs. RFP141C was constructed as a 42-mer peptide, and its compact molecular size enabled successful standard peptide synthesis. The compact RFP141C peptide could be stored as a powder, offering significant advantages for creating ARFs, including easy handling, transportability, and minimal/no lot-to-lot variations when creating ARFs.

In conclusion, the present work provided the first documented structural study on human RFP141C. We revealed that the C-terminal zinc finger possesses a unique compact RING fold for creating ARFs.

Methods

Peptide synthesis

The RFP141C peptide was constructed as RFP141C, which was identified via the SMART database. The ^{13}C- and ^{15}N-labeled RFP141C peptide was uniformly prepared with C-terminal amidation by standard F-moc solid-phase synthesis. Chemicals for peptide assembly, including amide resin, were obtained from Shimadzu Corp. (Kyoto, Japan) and Sigma-Aldrich Co. LLC (St Louis, MO, USA). After cleavage with trifluoroacetic acid, the peptide was purified using reversed-phase high-performance liquid chromatography with a Shim-pack C18 column (Shimadzu Corp.). Peptide purity was more than 98%, and the molecular mass of the RFP141C peptide was assessed by matrix-assisted laser desorption ionization-time of flight mass spectrometry on Shimadzu AXIMA-TOF2. The obtained peptide was dissolved in 0.36 mL of 8 *M* guanidine–HCl, and it was subsequently dialyzed against a degassed solution [20 m*M* Tris–HCl (pH 6.9), 50 m*M* NaCl, 1 m*M* dithiothreitol, and 50 μ*M* $ZnCl_2$] overnight at 4°C using Slide-A-Lyzer Dialysis Cassette (PIERCE).[15]

Stoichiometry of released zinc ions

The concentration of the RFP141C peptide was spectrophotometrically estimated by the Bradford method using bovine serum albumin as the standard. Zinc ions of the RFP141C peptide were released by PHMB and then quantified using the metallochromic indicator PAR. Absorbance values of the Zn^{2+}–PAR_2 complex at 20°C were recorded at 500 nm. The concentration of zinc ions was calculated using the equation $A = \varepsilon cl$, where ε represents the molar absorptivity and is $6.6 \times 10^4\ M^{-1}\ cm^{-1}$, l represents the cell length and is 1.0 cm, and c represents the molecular concentration. The molar ratio of zinc:protein was estimated based on the amount of released zinc ions and the RFP141C peptide.[19–21]

NMR spectroscopy

For NMR, the RFP141C peptide (1 mM) was dissolved in $^1H_2O/^2H_2O$ (9:1) in 20 m*M* Tris-d_{11}–HCl buffer (pH 6.9) (C/D/N Isotopes, Canada) containing 50 m*M* NaCl, 1 m*M* 1,4-$_{DL}$-dithiothreitol-d_{10}, and 50 μ*M* $ZnCl_2$.[30,31] All NMR measurements were performed at 20°C on Bruker AVANCE 500 MHz equipped with a cryogenic probe and an AVANCE 800 spectrometer using the WATERGATE pulse sequence.[32] Backbone resonance assignments of the peptide were obtained by standard triple-resonance experiments.[22] Assignments of side chains were achieved using HBHA-CONH, HCCCONNH, CCCONNH, HCCH–TOCSY, and HCCH–COSY spectra. The three-dimensional ^{15}N- and ^{13}C-edited NOESY spectra were recorded with mixing times of 80–120 ms. Aromatic ring resonances were assigned by HCCH–COSY and ^{13}C-edited NOESY spectra. The spectra were processed using NMRPipe,[33] and NMRView[34] was used for optimal visualization and spectral analysis.

Structure calculation

Peak lists for the ^{15}N- and ^{13}C-edited NOESY spectra were generated by the peak picking and integration functions of NMRView. Stereospecific assignments of

the methyl groups of Val and Leu were used when they were distinguishable in the NOESY pattern. The tetrahedral zinc coordination was made using the constraints of lower and upper distance limits with force constants of 500 kcal mol^{-1} $Å^{-1}$ (Zn–S_γ, Zn–C_β, and S_γ–S_γ for Cys and Zn–$N_{\delta 1}$ and S_γ–$N_{\delta 1}$ for His).[35,36] Automated NOE crosspeak assignments and structure calculations with torsion angle dynamics were performed using CYANA 2.1.[25] Structure calculations were started with 100 randomized conformers, and the standard CYANA-simulated annealing protocol was used with 10,000 torsion angle dynamics steps per conformer. Dihedral angle and hydrogen bond constraints were not used for structure calculations. For energy minimization, the 20 conformers with the lowest CYANA target function values were subjected to the Smart Minimizer algorithm (max steps 200, RMS gradient 0.01) in Discovery Studio 2.1 (Accelrys Software).[15] The obtained structures were checked using PROCHECK-NMR[26]. The Connolly surfaces of the structures were simulated using Discovery Studio 2.1. MOLMOL[37] was used to analyze the resulting 20 conformers.

Protein data bank accession number. The atomic coordinates (code 5XEK) have been deposited in the Protein Data Bank, Research Collaboratory for Structural Bioinformatics.

ACKNOWLEDGMENTS

The authors would like to thank Dr. Yoshitsugu Shiro, RIKEN SPring-8 Center, for the NMR instrumentation.

REFERENCES

1. Zheng N, Wang P, Jeffrey PD, Pavletich NP (2000) Structure of a c-Cbl-UbcH7 complex: RING domain function in ubiquitin-protein ligases. Cell 102:533–539.
2. Pascual J, Martinez-Yamout M, Dyson HJ, Wright PE (2000) Structure of the PHD zinc finger from human Williams–Beuren syndrome transcription factor. J Mol Biol 304:723–729.
3. Misra S, Hurley JH (1999) Crystal structure of a phosphatidylinositol 3-phosphate-specific membrane-targeting motif, the FYVE domain of Vps27p. Cell 97: 657–666.
4. Legge GB, Martinez-Yamout MA, Hambly DM, Trinh T, Lee BM, Dyson HJ, Wright PE (2004) ZZ domain of CBP: an unusual zinc finger fold in a protein interaction module. J Mol Biol 343:1081–1093.
5. Joazeiro CA, Weissman AM (2000) RING finger proteins: mediators of ubiquitin ligase activity. Cell 102:549–552.
6. Lorick KL, Jensen JP, Fang S, Ong AM, Hatakeyama S, Weissman AM (1999) RING fingers mediate ubiquitin-conjugating enzyme (E2)-dependent ubiquitination. Proc Natl Acad Sci USA 96:11364–11369.
7. Weissman AM (2001) Themes and variations on ubiquitylation. Nat Rev Mol Cell Biol 2:169–178.
8. Brzovic PS, Rajagopal P, Hoyt DW, King MC, Klevit RE (2001) Structure of a BRCA1–BARD1 heterodimeric RING–RING complex. Nat Struct Biol 8:833–837.
9. Katoh S, Tsunoda Y, Murata K, Minami E, Katoh E (2005) Active site residues and amino acid specificity of the ubiquitin carrier protein-binding RING-H2 finger domain. J Biol Chem 280:41015–41024.
10. Scheel H, Hofmann K (2003) No evidence for PHD fingers as ubiquitin ligases. Trends Cell Biol 13:285–287; author reply 287–288.
11. Miyamoto K, Sumida M, Yuasa-Sunagawa M, Saito K (2017) Highly sensitive detection of E2 activity in ubiquitination using an artificial RING finger. J Pept Sci 23:222–227.
12. Takenokuchi M, Miyamoto K, Saigo K, Taniguchi T (2015) Bortezomib causes ER stress-related death of acute promyelocytic leukemia cells through excessive accumulation of PML–RARA. Anticancer Res 35:3307–3316.
13. van Ree JH, Jeganathan KB, Malureanu L, van Deursen JM (2010) Overexpression of the E2 ubiquitin-conjugating enzyme UbcH10 causes chromosome missegregation and tumor formation. J Cell Biol 188:83–100.
14. Wu X, Zhang W, Font-Burgada J, Palmer T, Hamil AS, Biswas SK, Poidinger M, Borcherding N, Xie Q, Ellies LG, Lytle NK, Wu LW, Fox RG, Yang J, Dowdy SF, Reya T, Karin M (2014) Ubiquitin-conjugating enzyme Ubc13 controls breast cancer metastasis through a TAK1-p38 MAP kinase cascade. Proc Natl Acad Sci USA 111:13870–13875.
15. Miyamoto K (2014) Structural model of ubiquitin transfer onto an artificial RING finger as an E3 ligase. Sci Rep 4:6574.
16. Miyamoto K, Togiya K (2010) The creation of the artificial RING finger from the cross-brace zinc finger by alpha-helical region substitution. Biochem Biophys Res Commun 394:972–975.
17. Miyamoto K (2012) Ubiquitination of an artificial RING finger without a substrate and a tag. J Pept Sci 18:135–139.
18. Zhang S, Qiu W, Wu H, Zhang G, Huang M, Xiao C, Yang J, Kamp C, Huang X, Huellen K, Yue Y, Pan A, Lebo R, Milunsky A, Vogt PH (2001) The shorter zinc finger protein ZNF230 gene message is transcribed in fertile male testes and may be related to human spermatogenesis. Biochem J 359:721–727.
19. Hunt JB, Neece SH, Schachman HK, Ginsburg A (1984) Mercurial-promoted Zn^{2+} release from *Escherichia coli* aspartate transcarbamoylase. J Biol Chem 259:14793–14803.
20. Hunt JB, Neece SH, Ginsburg A (1985) The use of 4-(2-pyridylazo) resorcinol in studies of zinc release from *Escherichia coli* aspartate transcarbamoylase. Anal Biochem 146:150–157.
21. Shang Z, Liao YD, Wu FY, Wu CW (1989) Zinc release from Xenopus transcription factor IIIA induced by chemical modifications. Biochemistry 28:9790–9795.
22. Clore GM, Gronenborn AM (1994) Multidimensional heteronuclear nuclear magnetic resonance of proteins. Methods Enzymol 239:349–363.
23. Kornhaber GJ, Snyder D, Moseley HN, Montelione GT (2006) Identification of zinc-ligated cysteine residues based on 13Calpha and 13Cbeta chemical shift data. J Biomol NMR 34:259–269.
24. Sudmeier JL, Bradshaw EM, Haddad KE, Day RM, Thalhauser CJ, Bullock PA, Bachovchin WW (2003) Identification of histidine tautomers in proteins by 2D 1H/13C(delta2) one-bond correlated NMR. J Am Chem Soc 125:8430–8431.

25. Guntert P (2004) Automated NMR structure calculation with CYANA. Methods Mol Biol 278:353–378.
26. Laskowski RA, Rullmannn JA, MacArthur MW, Kaptein R, Thornton JM (1996) AQUA and PROCHECK-NMR: programs for checking the quality of protein structures solved by NMR. J Biomol NMR 8: 477–486.
27. Barlow PN, Luisi B, Milner A, Elliott M, Everett R (1994) Structure of the C3HC4 domain by 1H-nuclear magnetic resonance spectroscopy. A new structural class of zinc-finger. J Mol Biol 237:201–211.
28. Joazeiro CA, Wing SS, Huang H, Leverson JD, Hunter T, Liu YC (1999) The tyrosine kinase negative regulator c-Cbl as a RING-type, E2-dependent ubiquitin-protein ligase. Science 286:309–312.
29. Yokouchi M, Kondo T, Sanjay A, Houghton A, Yoshimura A, Komiya S, Zhang H, Baron R (2001) Src-catalyzed phosphorylation of c-Cbl leads to the interdependent ubiquitination of both proteins. J Biol Chem 276:35185–35193.
30. Miyamoto K, Togiya K, Kitahara R, Akasaka K, Kuroda Y (2010) Solution structure of LC5, the CCR5-derived peptide for HIV-1 inhibition. J Pept Sci 16: 165–170.
31. Miyamoto K, Togiya K (2011) Solution structure of LC4 transmembrane segment of CCR5. PLoS ONE 6: e20452.
32. Piotto M, Saudek V, Sklenar V (1992) Gradient-tailored excitation for single-quantum NMR spectroscopy of aqueous solutions. J Biomol NMR 2:661–665.
33. Delaglio F, Grzesiek S, Vuister GW, Zhu G, Pfeifer J, Bax A (1995) NMRPipe: a multidimensional spectral processing system based on UNIX pipes. J Biomol NMR 6:277–293.
34. Johnson BA (2004) Using NMRView to visualize and analyze the NMR spectra of macromolecules. Methods Mol Biol 278:313–352.
35. Wang B, Alam SL, Meyer HH, Payne M, Stemmler TL, Davis DR, Sundquist WI (2003) Structure and ubiquitin interactions of the conserved zinc finger domain of Npl4. J Biol Chem 278:20225–20234.
36. Tamames B, Sousa SF, Tamames J, Fernandes PA, Ramos MJ (2007) Analysis of zinc-ligand bond lengths in metalloproteins: trends and patterns. Proteins 69: 466–475.
37. Koradi R, Billeter M, Wuthrich K (1996) MOLMOL: a program for display and analysis of macromolecular structures. J Mol Graph 14:51–55. 29–32.